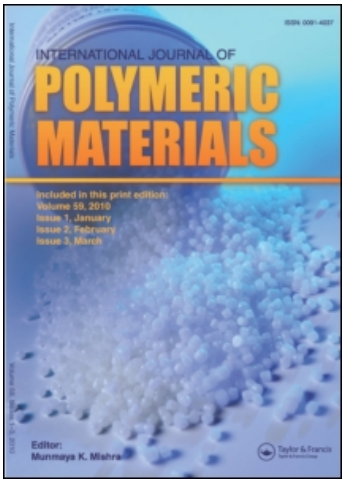

International Journal of Polymeric Materials

Publication details, including instructions for authors and subscription information:
http://www.informaworld.com/smpp/title~content=t713647664

Large Deformation Creep Behavior of a Solid Polymer

G. Rizzo[a]; G. Titomanlio[a]
[a] Instituto di Ingegneria Chimica, Università di Palermo, Italy

To cite this Article Rizzo, G. and Titomanlio, G.(1981) 'Large Deformation Creep Behavior of a Solid Polymer', International Journal of Polymeric Materials, 9: 1, 9 — 19
To link to this Article: DOI: 10.1080/00914038108077962
URL: http://dx.doi.org/10.1080/00914038108077962

Intern. J. Polymeric Mater., 1981, Vol. 9, pp. 9–19
0091–4037/81/0901–0009 $06.50/0

Printed in Great Britain

Large Deformation Creep Behavior of a Solid Polymer

G. RIZZO and G. TITOMANLIO
Instituto di Ingegneria Chimica, Università di Palermo, Italy

(*Received March 18, 1980*)

The effect of loading rate and strain on the creep behavior after sample yielding has been studied in previous communications (14–15) for Mylar in tension and for Lexan in compression. In this work the creep behavior of Lexan samples previously elongated is considered both in tension and in compression. A procedure which collects all the data independently of both loading rate and initial creep strain is proposed.

INTRODUCTION

The use of solid polymers as structurally efficient materials and the analysis of cold forming techniques requires the knowledge of their mechanical behavior above the linear viscoelasticity limit.

Numerous equations describing either on a theoretical basis or empirically the non linear creep have been proposed (see for instance Refs. 1–13). These equations are limited to relatively small strains. Only recently the creep behavior after deformations larger than the yield deformation has been considered in some detail both for Mylar in tensile tests[14] and for Lexan in compression.[15]

The results reported in Refs. 14–15 show that after yielding, the creep deformation depends remarkably on the sample loading rate and a much greater strain dependence was observed for Lexan in compression than for Mylar in tension.

In this work the creep at deformations larger than the yield deformation is further investigated on the same material considered in (15). The behavior of elongated samples both in tension and in compression is studied with the aim of obtaining a general correlation.

EXPERIMENTAL

Constant force creep tests were performed after constant velocity strain ramps both in tension and compression. All data were obtained at room temperature (about 20°C) by means of an Instron testing machine (mod. 1115) and the strain was measured by means of a transducer connected to the machine cross-head.

The material used was Lexan, a bisphenol A polycarbonate (4-4′dioxydiphenyl-2,2-propane carbonate) manufactured by General Electric. An average molecular weight of 25000 was determined by means of intrinsic viscosity measurements conducted at 20°C in chloroform. The material was supplied in the form of a rod and the absence of any shrinkage after heating up to 160°C above its glass transition temperature was assumed as a demonstration that it was in a non-oriented configuration, free of internal stresses.

The compression tests were performed on samples previously elongated. Cylindrical samples (with both height and diameter equal to about 7 mm) were obtained from the deformed portion of dumbbell shaped specimens subjected to elongation at room temperature up to the complete propagation of necking, which took place with a draw ratio of about 1.7. Compression creep tests could thus be performed at initial creep strains $e_c \equiv l_{oc}/l_o$ larger than one (where l_o indicates the original non-oriented sample height and l_{oc} indicates the sample height at the end of the constant velocity loading ramp, when the load reaches its final constant value). Data were taken on these samples for several values of the loading rate and of the initial creep strain after the sample yielding.

Some compression molded sheets, about 1.5 mm thick, were obtained from a portion of the original rod. These sheets were cold rolled in order to avoid necking of the material during subsequent elongation. Tensile creep tests after sample yielding could thus be performed at strains l_{oc}/l_o smaller than that which corresponds to the necking of non-oriented material. The rolling was done on a 2-roll mill having 7 cm diameter rolls 15 cm long. The rolls gap was reduced 0.01 mm per pass through the rolls. The rolling was performed up to two values of thickness reduction which correspond to deformations indicated as A and B in table I where the deformations along the width are also indicated. The deformations reported in Table I are only averages for each sheet, in fact the length increase changed about 6% along the width of the sheet. Samples were cut along the rolling direction from the sheets indicated by A in Table I and along the width direction from the sheets indicated by B. They were subjected to creep tests in tension at deformations larger than their yield deformation. During the tests the deformation of these samples was not isotropic and in particular, as expected, the thickness reduction was always smaller than the width reduction. For this reason the sample

TABLE I

Deformations achieved after rolling of compression molded sheets

	Increase factor in the rolling direction	Increase factor in the width direction
A	1.15	1.03
B	1.51	1.08

width, w_{oc}, and thickness, t_{oc}, at the end of the loading ramps had to be determined; the first one photographically and the second one, neglecting the density changes during the deformation, from the values of l_{oc} and w_{oc}.

RESULTS AND DISCUSSION

A. Stress-strain

The stress-strain behavior during constant velocity compression tests of samples elongated as described in the previous section are reported in Figure 1 as stress σ versus the strain $e \equiv l/l_o$ where l is the sample height (and l_o the

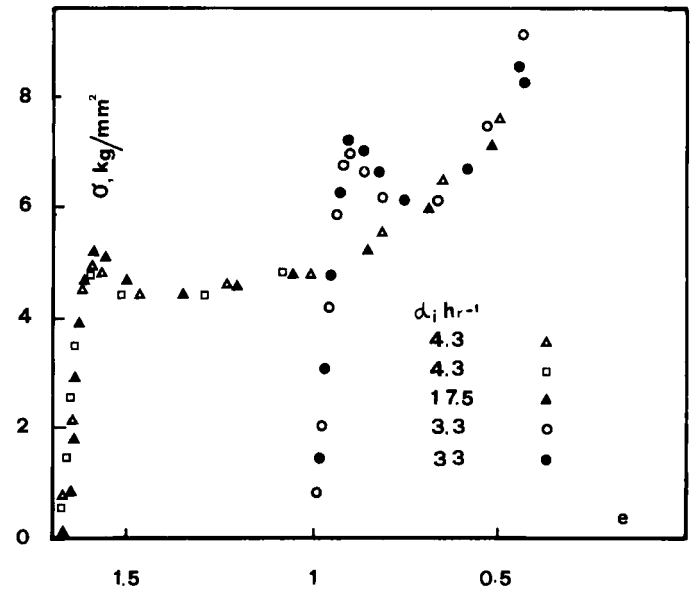

FIGURE 1 Stress σ *vs.* strain e during constant velocity compression tests. Both non-oriented and previously elongated samples are considered. α_i is initial deformation rate.

height of the original, non-oriented samples). Since these samples were previously elongated, the initial test strain (at beginning of the compression) $e_i = l_i/l_o$ is larger than one. In the same figure, stress-strain curves of non-oriented samples, $e_i = 1$, are also reported for comparison. The elongated samples (consistent with the Buashinger effect)[16] have a considerably smaller yield stress and their curves join those of the non-oriented samples soon after l/l_o becomes smaller than one.

B. Compression creep

The results of some compression constant force creep tests are plotted in Figure 2 as $\Delta l/l_{oc}$ (where Δl is the sample deformation as measured starting the instant when the prefixed load level had been reached) versus the time t. In the limit of small creep deformations, $\Delta l/l_{oc}$ coincides with the logarithmic strain $\ln(l/l_{oc})$. All the results reported in this figure refer to tests conducted with initial creep strains $e_c > 1$. Some tests performed at $e_c < 1$ on the same samples reproduced the results obtained[15] on non-oriented samples, $e_i = 1$, for the same value of both e_c and the deformation rate α_c just prior to the creep.

Analogously to what was observed with non-oriented samples[15] the data of Figure 2 show that the creep deformation is strongly influenced by the initial loading rate $\alpha_i \equiv v/l_i$ (where v is the velocity of the machine cross-head). Two curves relative to the same initial creep strain, e_c, and to different loading rates may be superimposed by means of a shift, on the log time axis, proportional to the loading rate. Much smaller is the effect of e_c which, for the data of Figure 2, is varied within a rather limited range. Some tests were performed changing the cross-head velocity during the loading; these data showed that, analogously to what was observed with the non-oriented samples, the creep behavior depends on the deformation rate $\alpha_c \equiv v/l_{oc}$ just prior to the test and thus α_c has to be considered in the time shift factor mentioned above.

Creep data taken in the range $0.7 \geqslant e_c \geqslant 0.3$ could be superimposed[15] by plotting the strain $\Delta l/l_{oc}$ versus the dimensionless time

$$\vartheta = t\alpha_c e_c \tag{1}$$

The data of Figure 2 and the two curves extremes of the data collected in (15) are reported in Figure 3 in terms of these coordinates. Although within each set of data, those with $e_c \leqslant 0.7$ and those at larger e_c values, the superposition may be considered satisfactory, the over all picture requires further adjustments. In particular focusing attention on small times, where the slope is larger and therefore horizontal shifts are more relevant, the curves at larger e_c, provided $e_c \geqslant 0.7$, need to be shifted to the left with respect to those at smaller e_c. Taking out, in this zone, e_c from Eq. 1 would produce a rearrange-

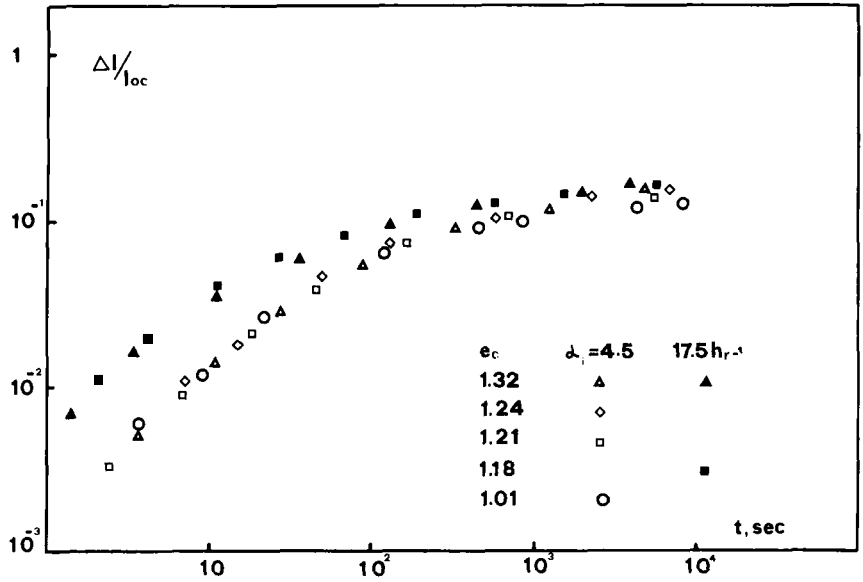

FIGURE 2 Creep strain under constant load in compression of samples previously elongated. α_i is the initial loading deformation rate. e_c is initial creep strain with respect to the non-oriented configuration.

ment sufficient to superimpose (at small times), the curves with $e_c \geqslant 0.7$. Similar indications where drawn in (14) where tensile constant force creep data taken at large strains on Mylar could be reduced into a single curve by means of a normalized time

$$\vartheta' = t\alpha_c \tag{2}$$

C. Tensile creep

The tensile creep data taken on rolled material are shown in Figure 4. Samples taken from sheets with both degrees of thickness reduction (A and B in Table I) are considered. Although both series of samples have about the same initial test strain along the testing direction (which is the rolling direction for samples of series A and the width direction for samples of series B) they have remarkably different initial strains along the other directions. In spite of this difference, the two series of samples showed very similar creep behavior especially at small times; in other words the creep behavior seems to depend essentially upon the strain e_c along the load direction. The effect of loading rate for these samples is identical to that observed in compression, that is, for a fixed initial creep strain, two creep curves may be superimposed by means of a time shift factor proportional to the strain rate just prior to the

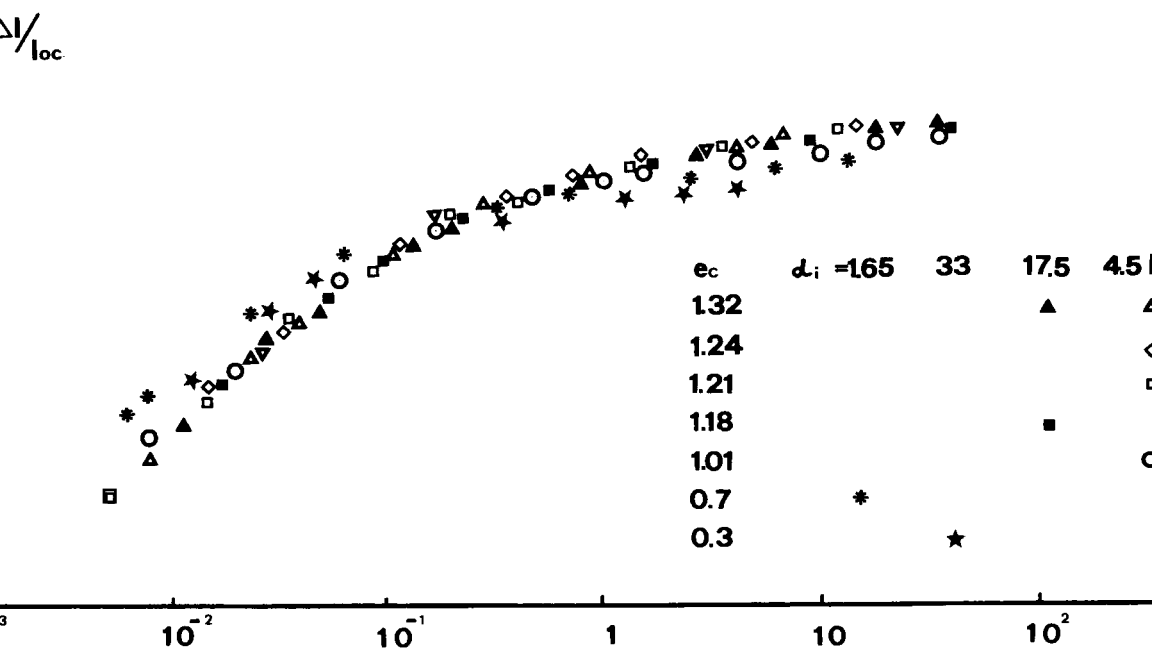

E 3 Constant load compression creep strain *vs.* the dimensionless time ϑ as defined by Eq. 1. α_i is initial deformation rate
ain with respect to the non-oriented configuration.

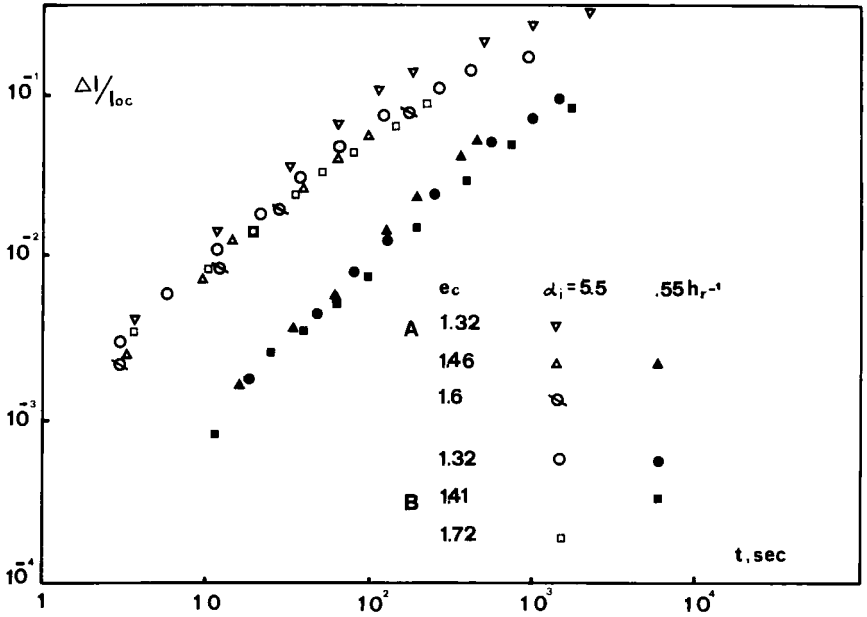

FIGURE 4 Constant load tensile creep of rolled samples. The rolling deformations of samples A and B are given in Table I. α_i is the initial loading deformation rate. e_c is the initial creep strain along the load direction with respect to the non-oriented configuration.

creep. Although, for a given loading rate, the effect of the initial creep strain is very small, within each series of samples of Figure 4 it may be observed that smaller values of e_c give rise to slightly faster creep deformation. In particular, because α_c decreases as e_c increases, also in this case, as observed above for the compression tests conducted at $e_c > 0.7$ and for Mylar in tension,[14] the use of the dimensionless time ϑ', as defined by Eq. 2, would produce an exact superposition of the data.

D. Overall correlation

In conclusion, in order to obtain a single creep curve, which considers simultaneously all the data at least at small creep deformations, one needs to replace e_c in Eq. 1 with a measure of strain which for $e_c < 0.7$ degenerates into e_c itself and for larger values of e_c is constant. Furthermore the data taken on the rolled samples suggest that this measure also needs to be more sensitive to the strain along the test direction than to the other strain components. At large times a complete superposition cannot be expected because, the tests being conducted at constant load, the stress increases with the creep deformation for the tensile tests and decreases for the compression tests.

In a RCCS the inverse of the Cauchy strain tensor of the present configuration with respect to the non-oriented configuration is defined as follows:[17]

$$[C_u^{-1}]^{i,j} = \frac{\partial X_u^i \partial X_u^j}{\partial X^m \partial X^m} \tag{3}$$

where X^m is the coordinate position of a material element in the present configuration and X_u^i is the coordinate position of the same element in the non-oriented configuration.

Identifying, in our case, X^1 with the load direction, one has

$$[C_u^{-1}]^{i,j} = \begin{vmatrix} 1/e_1^2 & 0 & 0 \\ 0 & 1/e_2^2 & 0 \\ 0 & 0 & 1/e_3^2 \end{vmatrix} \tag{4}$$

where the e_i are the ratios between the present sample dimension and the dimension of the non-oriented material along the ith direction.

At the instant when the creep begins the e_i are given by

$$\begin{aligned} e_1 &= e_c \\ e_2 &= e_{2,c} \equiv w_{oc}/w_o \\ e_3 &= e_{3,c} \equiv t_{oc}/t_o \end{aligned} \tag{5}$$

and the square root of the second invariant of $\mathbf{C}_u^{-1}$ is given by

$$\frac{1}{\sqrt{\text{II}C_u^{-1}}} = \frac{1}{\sqrt[4]{\dfrac{1}{e_c^4} + \dfrac{1}{e_{2,c}^4} + \dfrac{1}{e_{3,c}^4}}} \tag{6}$$

It can be shown that this quantity satisfies the requirements, specified above, to replace e_c in Eq. 1, giving rise to the following dimensionless time

$$\vartheta'' \equiv t\alpha_c/\sqrt{\text{II}C_u^{-1}} \tag{7}$$

All the data of Figure 4 and the two curves extremes (in terms of $\Delta l/l_{oc}$ and ϑ'') obtained from the data of Figure 3 are plotted again in Figure 5 using ϑ'' as dimensionless time. At relatively small times the superposition is certainly good; at larger times the data relative to tensile creep tests remain sensibly above those relative to compressive tests. As mentioned above, this is due to the fact that constant load means a stress decreasing (with the creep deformation) in compression and increasing in tension. Obviously this effect increases as the creep deformation proceeds. Furthermore at larger times, within each set of data (those in tension and those in compression), the superposition is not as good as at small times. The differences left however cannot only be accounted for by means of a time shift factor.

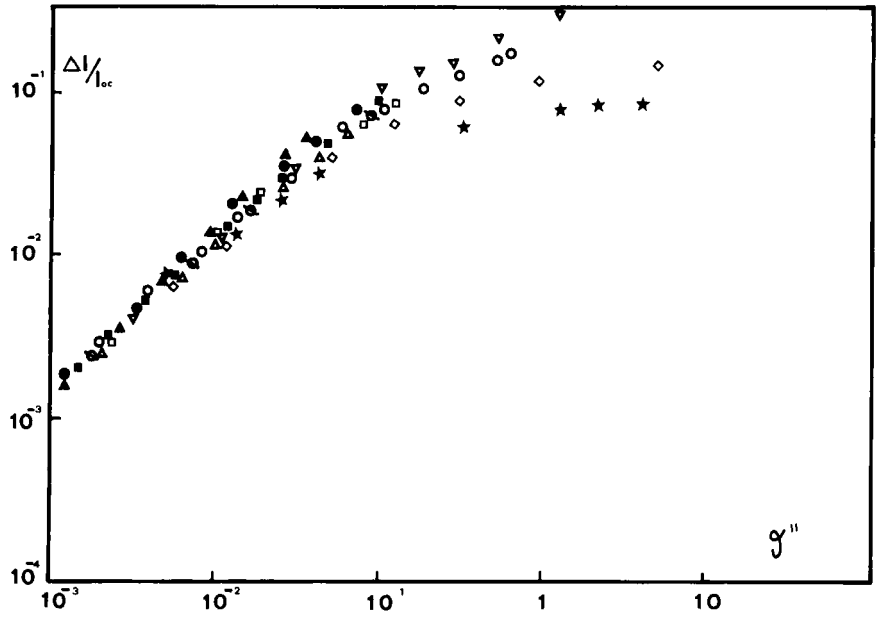

FIGURE 5 Both tensile and compression creep strain *vs.* the dimensionless time ϑ'' as defined by Eq. 7. Key to symbols as in Figure 4 except for ◇ ★, which refer to Figure 3.

CONCLUSIONS

Constant load creep data taken on Lexan, after the material yielding, both in tension and compression have been presented here. In particular the effect of loading rate, which in terms of deformation rate at the end of the strain ramp has been varied over a one hundred fold-range, and of the initial creep strain as referred to the non-oriented material configuration have been analyzed.

A superposition rule, which at small times collects all the data into a single curve, is proposed. At larger times the data taken under tensile load remain somewhat above those taken in compression. The proposed rule, accounting for strain by means of an invariant measure of it, may be applied also to materials which have complex deformations frozen in and furthermore is coherent also with previous results obtained on Mylar under tensile loading.

The correlation mentioned above has been here tested only by means of samples having either uniaxial or biaxial strain, the load being applied along one of the principal strain directions. Strictly, creep data taken under different strain situations should be analyzed before being allowed to consider the procedure for general use.

Should this be verified, the creep behavior for any value of the loading rate

and of the initial creep strain (no matter how complex it is) could be determined by means of a single creep test performed at deformations larger than the yield deformation.

LIST OF SYMBOLS

$\mathbf{C}_u^{-1}$	The inverse of the Cauchy strain tensor, assuming as reference the non-oriented configuration, see Eq. 3
${}^{II}C_u^{-1}$	Second invariant of $\mathbf{C}_u^{-1}$
e	Sample strain along the loading direction, assuming as reference the non-oriented configuration
e_c	Value of e when the creep load is reached
e_i	Value of e before loading the sample
e_1, e_2, e_3	Strains along principal directions
$e_{2,c}, e_{3,c}$	See Eq. 5
l	Sample height
Δl	Sample height variation as measured since the creep load is reached
l_i	Value of l before loading the sample
l_0	Value of l in the non-oriented configuration
l_{oc}	Value of l when the creep load is reached
RCCS	Rectangular cartesian coordinates system
t	Time as measured since the creep load is reached
t_0	Sample thickness in the non-oriented configuration
t_{oc}	Sample thickness when the creep load is reached
v	Machine cross-head velocity
w_0	Sample width in the non-oriented configuration
w_{oc}	Sample width when the creep load is reached
X^m	Coordinate position of a material element in the present configuration
X_u^i, X_u^j	Coordinate position of a material element in the non-oriented configuration
α_c	Deformation rate when the creep load is reached
α_i	Deformation rate at the beginning of the loading ramp
ϑ	Dimensionless time, as defined by Eq. 1
ϑ'	Dimensionless time, as defined by Eq. 2
ϑ''	Dimensionless time, as defined by Eq. 7
σ	True stress

Acknowledgement

This work has been supported by C. N. R. Grant No. 78.00935.03. Thanks are due to Mr. G. Comandè for drawing of figures.

References

1. W. Kauzman and H. Eyring, *J. Amer. Chem. Soc.*, **62,** 3113 (1940).
2. W. N. Findley and G. Khosla, *J. Appl. Phys.*, **26,** 821 (1955).
3. O. Nokada, *J. Phys. Soc. Japan*, **15,** 2280 (1960).
4. M. G. Sharma and P. R. Wen, *Trans. SPE*, **4,** 282 (1964).
5. A. C. Pipkin and T. G. Rogers, *J. Mech. Phy. Solids*, **16,** 59 (1968).
6. L. E. Nielsen, *J. Appl. Polym. Sci.*, **13,** 1800 (1969).
7. I. V. Yannas, *J. Polym. Sci.*, **9,** 163 (1974).
8. L. E. Nielsen, *Trans. Soc. Rheol.*, **13,** 141 (1969).
9. S. Turner, *British Plast.*, **37,** 501 and 567 (1964).
10. R. P. Kambour and R. E. Robertson, *Polymer Science*, A. D. Jenkins, Ed. (North-Holland Publ., Amsterdam), Chap. 11.
11. I. H. Hall, *J. Polym. Sci.*, **A-2, 5,** 1119 (1967).
12. I. M. Ward and J. M. Wolf, *J. Mech. Phys. Solids*, **14,** 131 (1966).
13. C. J. Morgan and I. M. Ward, *J. Mech. Phys. Solids*, **19,** 165 (1971).
14. G. Titomanlio and G. Rizzo, *J. Appl. Polym. Sci.*, **21,** 2933 (1977).
15. G. Titomanlio and G. Rizzo, Compressive large deformation viscoelastic behavior of a polycarbonate, *Polymer*, **21,** 461 (1980).
16. R. N. Haward, *The Physics of Glassy Polymers* (Appl. Sci. Publ. Ltd., London) 1973.
17. G. Astarita and G. Marrucci, *Principles of Non-Newtonian Fluid Mechanics* (McGraw-Hill Book Co. Ltd., London) 1974.